

TAILORING A PAIR OF PANTS

HELGE RUDDAT AND ILIA ZHARKOV

ABSTRACT. We show that the complex pair of pants $P^\circ \subset (\mathbb{C}^*)^n$ is (ambient) isotopic to a natural polyhedral subcomplex of the product of the two skeleta $S \times \Sigma \subset \mathcal{A} \times \mathcal{C}$ of the amoeba \mathcal{A} and the coamoeba \mathcal{C} of P° . We thereby provide the groundwork to be able to isotope the discriminant into codimension 2 in topological SYZ torus fibrations.

1. INTRODUCTION

The $(n-1)$ -dimensional pair-of-pants P° is the main building block for many problems in complex and symplectic geometries. Its projection $\mathcal{A} \subset \mathbb{R}^n$ under the $\log|z|$ map is called the *amoeba* and its projection $\mathcal{C} \subset \mathbb{T}^n$ via the argument map is the *coamoeba*. Both \mathcal{A} and \mathcal{C} have well known skeleta: the spine $S^\circ \subset \mathcal{A}$, also known as the tropical hyperplane, and $\Sigma \subset \mathcal{C}$, whose cover is the boundary of the A_n -permutahedron. It is convenient to compactify $(\mathbb{C}^*)^n$ (and subspaces in it) to the product $\Delta \times \mathbb{T}^n$, where Δ is the standard n -simplex. We introduce a natural polyhedral complex $\mathcal{P} \subset \Delta \times \mathbb{T}^n$, the *ober-tropical* pair-of-pants, which is a subcomplex of $S \times \Sigma$. Its projection to S has equidimensional fibers with the center fiber being Σ . The main result of the paper Theorem 6 states that \mathcal{P} is (ambient) isotopic to P (in the PL category).

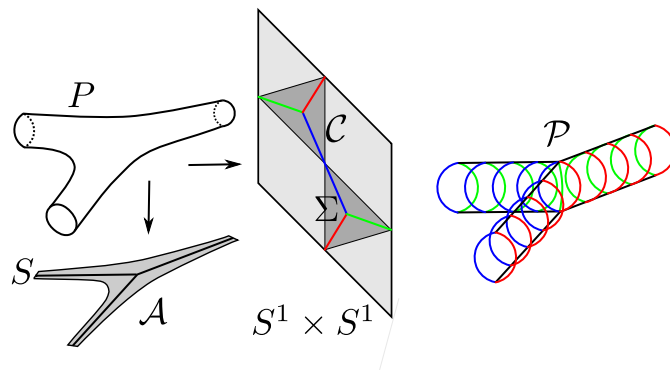


FIGURE 1. The ober-tropical subcomplex $\mathcal{P} \subset S \times \Sigma$ for $n = 2$.

The research of I.Z. is partially supported by the NSF FRG grant DMS-1265228 and Simons Collaboration grant A20-0125-001. H.R. was supported by DFG grant RU 1629/4-1 and the Department of Mathematics at Universität Hamburg.

One can easily visualize an isotopy for the one-dimensional pair of pants. But the simplicity of the $n = 2$ case is deceptive. To get a hint of how complicated the isotopy problem becomes in higher dimensions, consider a long pentagon (a point in the 3-dimensional pair of pants, $n = 4$). This pentagon maps to a point y in the face $S_{02} : |z_0| = |z_2| \gg |z_i|, i \neq 0, 2$

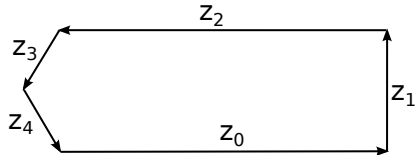


FIGURE 2. The tall house fallen.

in the spine S of the amoeba. On the other hand it maps to a point s in the face $\Sigma_{\langle 1,2340 \rangle}$ of the skeleton of the coamoeba (the average of the four arguments of z_0, z_2, z_3, z_4 is opposite to the argument of z_1). The problem is that, roughly speaking, the two acutest angles do not separate the two longest sides of the pentagon, so that $y \in S_{02}$ is “very far” from any legitimate strata in the fiber of $s \in \Sigma_{\langle 1,2340 \rangle}$. (This never happens for triangles because of the larger side lying against larger angle property). So the isotopy cannot be a “small deformation”.

Instead of trying to build an isotopy explicitly (which is an interesting but, perhaps, a rather difficult problem) we build regular cell decompositions of both pairs and show that they are homeomorphic. The cell structures respect the natural stratification of $\Delta \times \mathbb{T}^n$, so the homeomorphisms will glue well at the boundary. Thus with a little bit of effort the isotopy can be extended to any general affine hypersurface.

The isotopy we provide may be applied to several questions in mirror symmetry. One application we have in mind is the following. Given an integral affine manifold with simple singularities [GS06] we want to build a topological SYZ fibration [SYZ96] with discriminant in codimension 2 (rather than codimension one). So far the only examples are the K3 (with discriminant consisting of 24 points in S^2) and the quintic 3-fold [G01], cf. [CBM09, EM19]. In a general case, the idea is roughly to modify the local models of the fibration $\{w = f\} \subset X_\Sigma \times (\mathbb{C}^*)^{n-k}$. Here X_Σ is an affine toric variety with Σ a cone over some k -dimensional simplex Δ_1 , $w : X_\Sigma \rightarrow \mathbb{C}$ is a natural toric map, and $f : (\mathbb{C}^*)^{n-k} \rightarrow \mathbb{C}$ is a Laurent polynomial with a prescribed Newton polytope, a simplex Δ_2 . The local model has the structure of a T^k -bundle over $\mathbb{R}^k \times (\mathbb{C}^*)^{n-k}$ with fibers collapsing over $\mathcal{H}_1 \times H_2$ where \mathcal{H}_1 is the codimension one skeleton of the normal fan to Δ_1 , and $H_2 = \{f = 0\}$ is a hypersurface in $(\mathbb{C}^*)^{n-k}$. One then further projects to the \mathbb{R}^{n-k} -factor by the Log map in $(\mathbb{C}^*)^{n-k}$. To have the T^n -fibration $\{w = f\} \rightarrow \mathbb{R}^n$ with discriminant in codimension 2, we can use our isotopy to replace the pair $H_2 \subset (\mathbb{C}^*)^{n-k}$ with a pair $\mathcal{H}_2 \subset (\mathbb{C}^*)^{n-k}$ such that now \mathcal{H}_2 is mapped to the *spine* of the amoeba of H_2 . The details are in our forthcoming paper [RZ20].

Thanks. The authors would like to thank the organizers of the Tropical workshop at Oberwolfach in May 2019 where the second author came up with the new object \mathcal{P} for the

first time (hence the name). Our gratitude for hospitality additionally goes to the Mittag-Leffler institute, Institute of the Mathematical Sciences of the Americas and MATRIX in Creswick.

2. GEOMETRY OF THE COMPLEX PAIR OF PANTS

2.1. Notations. We set $\hat{n} := \{0, \dots, n\}$. We will think of $(\mathbb{C}^*)^n \cong (\mathbb{C}^*)^{n+1}/\mathbb{C}^*$ as the product $\Delta^\circ \times \mathbb{T}^n$ where Δ° is the interior of the n -simplex

$$\Delta := \left\{ (x_0, \dots, x_n) \in \mathbb{R}^{n+1} : x_i \geq 0, \sum x_i = 1 \right\}$$

and $\mathbb{T}^n := (\mathbb{R}/2\pi\mathbb{Z})^{n+1}/(\mathbb{R}/2\pi\mathbb{Z})$ is the n -torus with homogeneous coordinates $[\theta_0, \dots, \theta_n]$. It is more natural to work with closed spaces, especially for the gluing purposes, so we will compactly $(\mathbb{C}^*)^n$ to $\Delta \times \mathbb{T}^n$ and all subspaces in $(\mathbb{C}^*)^n$ by taking their closures in $\Delta \times \mathbb{T}^n$. We will denote by $\text{bsd } \Delta$ the first barycentric subdivision of Δ . We will also consider the

dualizing subdivision $\text{dsd } \Delta$ which is a coarsening of $\text{bsd } \Delta$ by combining all simplices in $\text{bsd } \Delta$ from a single interval $[I, J]$ together. That is, a cell Δ_{IJ} in $\text{dsd } \Delta$ is

$$\Delta_{IJ} := \text{Conv}\{\hat{\Delta}_K : I \subseteq K \subseteq J\},$$

where $\hat{\Delta}_K$ stands for the barycenter of Δ_K .

The dualizing subdivision can be applied to any polytope Q where it interpolates between the cone structure of the normal fan in the interior of Q and the original face stratification at the boundary of Q . For a general polytope Q the cells in $\text{dsd } Q$ need not be polytopes anymore, but it is still a regular CW-complex.

The **hypersimplex** $\Delta^n(2) \subset \Delta^n$ is obtained from the ordinary simplex by cutting the corners half-way. That is,

$$\Delta^n(2) := \{(x_0, \dots, x_n) \in \mathbb{R}^{n+1} : \sum x_i = 2\pi \text{ and } 0 \leq x_i \leq \pi\}.$$

We will use $2\pi = 1$ for the amoeba and $2\pi = 6.28\dots$ for the coamoeba.

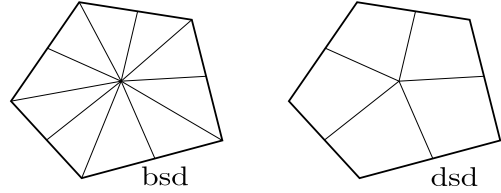
The **cyclic polytope** $C_d(r)$ is the convex hull of the points $x(t_1), \dots, x(t_r)$ in \mathbb{R}^d , where $x(t) = (t, t^2, \dots, t^d)$ and $t_1 < \dots < t_r$ are real numbers.

2.2. A cell decomposition of the complex pair of pants. The $(n-1)$ -dimensional **pair-of-pants** P° is the complement of $n+1$ generic hyperplanes in $\mathbb{C}\mathbb{P}^{n-1}$. By an appropriate choice of coordinates we can identify P° with the affine hypersurface in $(\mathbb{C}^*)^{n+1}/\mathbb{C}^*$ given in homogeneous coordinates by

$$z_0 + z_1 + \dots + z_n = 0.$$

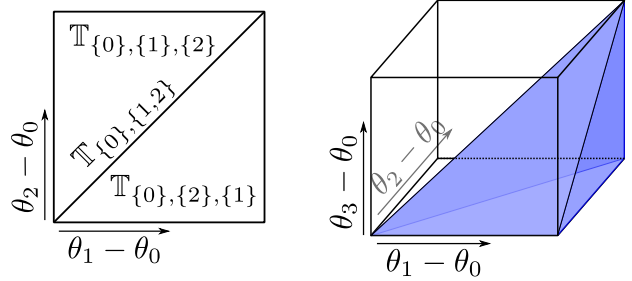
We define the **compactified pair-of-pants** P to be the closure of P° in $\Delta \times \mathbb{T}^n$ via the map

$$\mu_1 \times \mu_2 : (\mathbb{C}^*)^{n+1}/\mathbb{C}^* \rightarrow \Delta \times \mathbb{T}^n, \quad [z_0, \dots, z_n] \mapsto \left(\frac{|z_0|}{\sum |z_i|}, \dots, \frac{|z_n|}{\sum |z_i|}; [\arg z_0, \dots, \arg z_n] \right)$$



where we abused notation when writing the quotient of \mathbb{T}^{n+1} modulo the diagonal \mathbb{T}^1 simply by \mathbb{T}^n (with coordinates $\theta_1 - \theta_0, \dots, \theta_n - \theta_0$). The closure P is a manifold with boundary, and it can be thought of as a real oriented blow-up of $\mathbb{C}\mathbb{P}^{n-1}$ along its intersections with the coordinate hyperplanes in $\mathbb{C}\mathbb{P}^n$.

FIGURE 3. Stratification of the torus \mathbb{T}^n for $n = 2$ and $n = 3$. The right only shows $\mathbb{T}_{\{0,\{3\},\{2\},\{1\}}^3$ in blue and there exist five further maximal strata. Only zero-dimensional strata are closed.



Next we review a natural stratification $\{P_{\sigma,J}\}$ of P from [KZ18] induced from a product stratification of $\Delta \times \mathbb{T}^n$. The stratification $\{\Delta_J\}$ of the simplex Δ is given by its face lattice, namely by the non-empty subsets $J \subseteq \hat{n}$. The set of the hyperplanes $\theta_i = \theta_j$, $i, j \in \hat{n}$, stratifies the torus \mathbb{T}^n by cyclic orderings of the points $\theta_0, \dots, \theta_n$ on the circle. The strata \mathbb{T}_σ^n are labeled by **cyclic partitions** $\sigma = \langle I_1, \dots, I_k \rangle$ of the set \hat{n} , that is, $\hat{n} = I_1 \sqcup \dots \sqcup I_k$ and the sets I_1, \dots, I_k are cyclically ordered. The elements within each I_i are not ordered. We call the I_i the **parts** of σ and we set $|\sigma| := k$. If all parts are 1-element sets then we will write $\sigma = \langle i_0, \dots, i_n \rangle$.

We can view points in $P_{\sigma,J}$ as (degenerate) convex polygons in the plane defined up to rigid motions and scaling. The edges represent the complex numbers z_0, \dots, z_n ordered counterclockwise according to σ . The edges within each I_s are parallel and not ordered. The edges of the polygon which are not in J have zero length but their directions are still recorded.

Each \mathbb{T}_σ^n can be thought of as the interior of the simplex

$$(1) \quad \Delta_\sigma := \left\{ (\alpha_1, \dots, \alpha_k) \in \mathbb{R}^k : \alpha_i \geq 0, \sum \alpha_i = 2\pi \right\}$$

The coordinates α_i play the rôle of exterior angles of the convex polygons. The precise relation between α 's and the original arguments θ 's is as follows: $\theta_i = \theta_j$ for $i, j \in I_s$ and $\theta_i + \alpha_s = \theta_j$ for $i \in I_s, j \in I_{s+1}$. Here we assume the periodic indexing $I_{s+k} = I_s$.

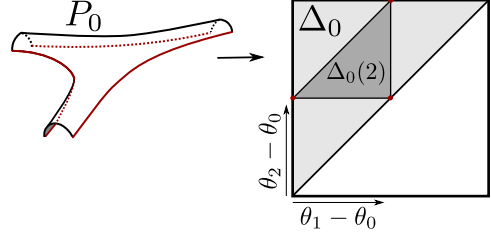
The inclusion of closed strata $P_{\sigma',J'} \subseteq P_{\sigma,J}$ gives a partial order among the pairs: $(\sigma', J') \preceq (\sigma, J)$ if σ is a refinement of σ' (we write $\sigma' \preceq \sigma$) and $J' \subseteq J$. To simplify notations we will drop the index J from the subscript if $J = \hat{n}$.

We have a natural surjection $\Delta_\sigma \rightarrow \overline{\mathbb{T}_\sigma^n}$ which is bijective away from the vertices (all the vertices map to $0 \in \mathbb{T}^n$). Since $P_{\sigma,J}$ does not have any points lying over the vertices

of Δ_σ , we may view $P_{\sigma,J}$ to be sitting as

$$P_{\sigma,J} \subseteq \Delta_J \times \Delta_\sigma.$$

We set $\sigma_0 = \langle 0, 1, \dots, n \rangle$ and $\Delta_0 := \Delta_{\sigma_0}$. For $J = \hat{n}$ and $\sigma = \sigma_0$ we denote the corresponding maximal stratum of P by $P_0 \subseteq \Delta \times \Delta_0$. All maximal strata are isomorphic to P_0 .



We say that σ **divides** J , and write $\sigma|J$, if

J contains elements in at least two of the subsets I_1, \dots, I_k of $\sigma = \langle I_1, \dots, I_k \rangle$. The face poset of a stratum $P_{\sigma,J}$ consists of pairs (σ', J') such that $\sigma' \preceq \sigma$, $J' \subseteq J$ and σ' divides J' . This, in particular, means that $|\sigma'| \geq 2$ and $|J'| \geq 2$. If σ does not divide J the stratum $P_{\sigma,J}$ is empty. The dimension of $P_{\sigma,J}$ is $|\sigma| + |J| - 4$.

To represent (σ, J) we will use the following **graphical code**. Once the maximal partition $\sigma_0 = \langle i_0, \dots, i_n \rangle$ is fixed, we may think of σ_0 as a cyclic labelling of the edges of the $(n + 1)$ -gon or equivalently a labelling of the $n + 1$ arcs on a circle separated by $n + 1$ vertices. Now every coarsening $\sigma \preceq \sigma_0$ can be represented as a subset V of the vertices, namely the set of vertices that separate two consecutive parts in σ . Furthermore, we view J as a subset of the edges (or arcs). Consequently, we may represent (σ, J) as a circle with $n + 1$ vertices and $n + 1$ labeled arcs, out of which the arcs in J and the vertices in V have been marked. We graphically indicate an arc marking by connecting the adjacent vertices of the arc by a straight line, see Figure 4.

The σ -divides- J property now translates into saying that the pair (V, J) be **interlacing**, which means that not all edges in J are lying in an arc between two elements of V . We call a pair (V, J) **maximally interlacing** if it is interlacing and either every part of σ has an element from J (if $|\sigma| \leq |J|$) or every part of σ contains at most one element of J (if $|\sigma| \geq |J|$). The lowest strata of P_0 are the (maximal) interlacing pairs (V, E) where V is a pair of vertices and E is a pair of edges separated by V . A pair (V, E) is **maximal**

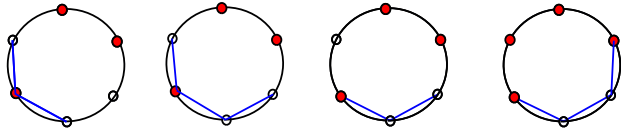


FIGURE 4. For $n + 1 = 6$, examples of graphical code referencing subsets (V, J) that are *maximal* and *non-maximal interlacing*, *non-interlacing*, and *maximal non-interlacing*. The vertex subsets are indicated by red coloring and the edge markings by blue segments.

non-interlacing if adding an extra element to either V or E will make it interlacing.

The following observation (cf. Conjecture 1 in [KZ18]) was suggested by Stanley [St19].

Proposition 1. *The face lattice of P_0 is dual to the face lattice of the cyclic polytope $C_{2n-2}(2n + 2)$.*

Proof. If we label the edges z_i of the polygon by t_{2i} and the vertices between z_i and z_{i+1} by t_{2i+1} then the interlacing condition for a minimal pair (V, E) is equivalent to that there are even number of t_j 's between any two consecutive elements of $\{t_{e_1}, t_{v_1}, t_{e_2}, t_{v_2}\}$. This confirms the Gale evenness condition (see, e.g. [Zi95, Theorem 0.7]), for the facets (our vertices) of the cyclic polytope. \square

The lower dimensional strata are isomorphic to the faces of P_0 and hence every lower interval $\mathcal{W}_{\preceq(\sigma, J)} := \{(\sigma', J') \in \mathcal{W} : (\sigma', J') \preceq (\sigma, J)\}$ is the face lattice of a polytope $C_{\sigma, J}^\vee$. In particular, the facets of P_0 are dual to the cyclic polytope $C_{2n-3}(2n+1)$.

Remark. The appearance of the rational normal curve in the picture seems very intriguing.

2.3. The amoeba and its skeleton. The image $\mathcal{A} := \mu_1(P) \subset \Delta$ is called the (compactified) **amoeba** of the hypersurface P [GKZ94]. It is easy to see that \mathcal{A} is the hypersimplex $\Delta(2)$, since the only restrictions on lengths of the z_i are given by the triangle inequalities. That is, if we normalize the perimeter to be 1, then \mathcal{A} is cut out by the inequalities $|z_i| \leq 1/2$.

The **skeleton** S of \mathcal{A} (also known as the spine or the tropical hyperplane) is a polyhedral subcomplex of Δ defined as

$$S = \{(x_0, \dots, x_n) \in \Delta : x_i = x_j \geq x_k \text{ for some } i \neq j \text{ and all } k \neq i, j\}.$$

The faces S_{IJ} of S are parameterized by pairs of subsets $I \subseteq J \subseteq \hat{n}$, such that $|I| \geq 2$. Namely, S_{IJ} is defined by $x_i = x_{i'} \geq x_k$ for all $i, i' \in I, k \notin I$ and $x_j = 0, j \notin J$. A well-known observation is the following.

Proposition 2. *The amoeba \mathcal{A} deformation retracts to its skeleton S .*

2.4. The permutahedron and the zonotope. Before we describe the coamoeba and its skeleton we review some notations and basic facts from the A_n -root system terminology. We write $\mathbb{R}^{n+1}/\mathbb{R}$ for the quotient space $\mathbb{R}^{n+1}/\mathbb{R}(1, \dots, 1)$. Let e_0, \dots, e_n be a basis of the Euclidean space $(\mathbb{R}^{n+1})^*$. The **roots** in $\Lambda_{\mathbb{R}} := (\mathbb{R}^{n+1}/\mathbb{R})^*$ are $\alpha_{ij} = e_i - e_j$. The inner product on $\Lambda_{\mathbb{R}}$ is induced from $(\mathbb{R}^{n+1})^*$. Over \mathbb{Z} the roots generate the **root lattice** $\Lambda \subset \Lambda_{\mathbb{R}}$.

The **weight lattice** $W \subset \Lambda_{\mathbb{R}}$ is the dual lattice to Λ with respect to the inner product. For any partition of \hat{n} into two non-empty subsets $\{I_-, I_+\}$, we define the **fundamental weight**

$$(2) \quad w_{I_-, I_+} = \frac{r}{n+1} \sum_{j \in I_+} e_j - \frac{s}{n+1} \sum_{i \in I_-} e_i \in W,$$

where $r = |I_-|$ and $s = |I_+| = n+1 - r$. Its length squared is

$$|w_{I_-, I_+}|^2 = \frac{sr^2 + rs^2}{(n+1)^2} = \frac{rs}{n+1}.$$

There are $2^{n+1} - 2$ fundamental weights.

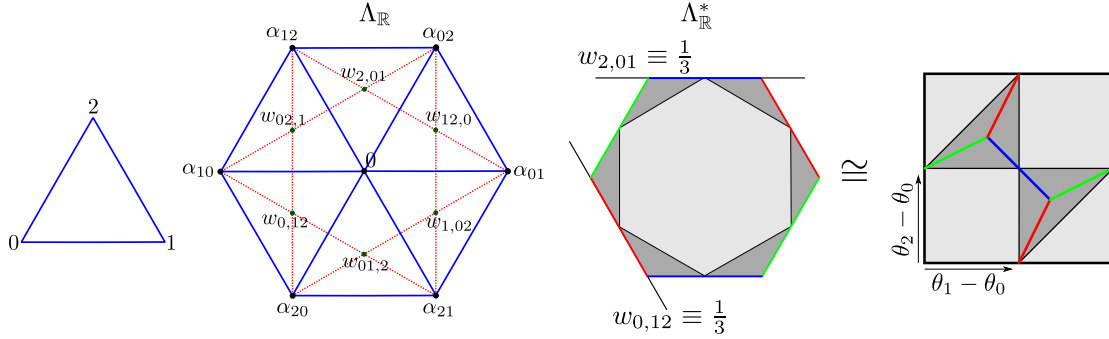


FIGURE 5. For $n = 2$: a choice of homogeneous coordinates of the triangle, the corresponding roots and fundamental weights, the permutohedron with zonotope inside and how these give rise to the coamoeba and its skeleton

The quadratic form $Q(w) = \pi|w|^2$ on W provides the **Delaunay triangulation** of $\Lambda_{\mathbb{R}}$ by looking at the convex upper hull of its graph. This triangulation is W -periodic. The edge vectors originating at 0 are the fundamental weights. The maximal simplices incident to 0 correspond to permutations $\{i_0, \dots, i_n\}$ of the set \hat{n} . Such a permutation determines a choice of positive and simple roots in Λ . Then the convex hull of the corresponding set of n **dominant** fundamental weights

$$(3) \quad \frac{1}{n+1}(-1, \dots, -1, n), \quad \frac{1}{n+1}(-2, \dots, -2, n-1, n-1), \quad \dots, \quad \frac{1}{n+1}(-n, 1, \dots, 1)$$

(written in the basis e_{i_0}, \dots, e_{i_n}) together with the origin gives a maximal Delaunay simplex. The cone they generate is known as the Weyl alcove.

More generally, the faces in the Delaunay triangulation (up to translations by W) are labeled by ordered partitions $\bar{\sigma} = \{I_1, \dots, I_k\}$ of \hat{n} . The single vertex (up to translations by W) corresponds to the 1-partition $\bar{\sigma} = \{\hat{n}\}$.

We now consider the dual space $\Lambda_{\mathbb{R}}^* = \mathbb{R}^{n+1}/\mathbb{R}$. The basis e_0, \dots, e_n defines homogeneous coordinates $[x_0, \dots, x_n]$ in $\Lambda_{\mathbb{R}}^*$. The **coweight lattice** Λ^* which is dual to Λ is naturally identified with the lattice $\mathbb{Z}^{n+1}/\mathbb{Z} \subset \mathbb{R}^{n+1}/\mathbb{R}$.

The A_n -type Delaunay triangulation of $\Lambda_{\mathbb{R}}$ is a **dicing** with respect to Λ . That is, it is given by a totally unimodular system of families of parallel hyperplanes (cf. [Er94]). An equivalent statement is that the dual decomposition of $\Lambda_{\mathbb{R}}^* = \mathbb{R}^{n+1}/\mathbb{R}$, known as the Voronoi tiling, is by zonotopes. This tiling is $2\pi\Lambda^*$ -periodic. Explicitly, the Voronoi tiles are the domains of linearity of the Legendre transform of $Q(w)$ – the convex quasi-periodic PL function on $\mathbb{R}^{n+1}/\mathbb{R}$:

$$\Theta(u) = \max_{w \in W} \{ \langle w, u \rangle - \pi|w|^2 \}.$$

Now let's go back to the skeleton. We denote by Perm the central maximal Voronoi tile (the one which contains 0 in its interior). Other maximal tiles are translations of Perm by elements in the lattice $2\pi\Lambda^*$. In homogeneous coordinates $[x_0, \dots, x_n]$ the central tile is

defined by the following inequalities:

$$(4) \quad -\frac{s}{n+1} \sum_{i \in I_-} x_i + \frac{r}{n+1} \sum_{j \in I_+} x_j \leq \frac{rs}{n+1} \pi,$$

one inequality per each fundamental weight w_{I_-, I_+} .

The vertices of Perm are in one-to-one correspondence with the maximal simplices of the Delaunay triangulation incident to 0. More precisely, the vertex of Perm corresponding to a permutation $\bar{\sigma} = \{i_0, \dots, i_n\}$ is given in homogeneous coordinates $[x_{i_0}, \dots, x_{i_n}]$ by

$$(5) \quad \rho_{\bar{\sigma}}^\vee = \frac{\pi}{n+1} [1, 3, \dots, 2n-1, 2n+1].$$

Indeed, we evaluate $\rho_{\bar{\sigma}}^\vee$ on the set of the dominants weights (3). The calculation for a weight

$$w_{I_-, I_+} = \left(\underbrace{-\frac{s}{n+1}, \dots, -\frac{s}{n+1}}_r, \underbrace{\frac{r}{n+1}, \dots, \frac{r}{n+1}}_s \right)$$

becomes more transparent if we represent $\rho_{\bar{\sigma}}^\vee$ by

$$\rho_{\bar{\sigma}}^\vee = \frac{\pi}{n+1} [-2r+1, -2r+3, \dots, -1, 1, \dots, 2s-1].$$

Then

$$\langle \rho_{\bar{\sigma}}^\vee, w_{I_-, I_+} \rangle = \frac{\pi}{(n+1)^2} (r^2 s + s^2 r) = \pi Q(w_{I_-, I_+}).$$

The vertices of Perm are permuted under the action of the symmetric group action, so Perm is indeed a permutahedron. But it is a very special one: it tiles the space.

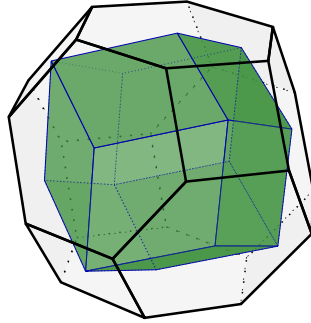


FIGURE 6. For $n = 3$: the permutahedron containing the zonotope

Proposition 3. *The zonotope $Z = \sum_{i=0}^n [0, \pi] e_i$ lies entirely in Perm. Moreover, the vertices of Z are the only points on the boundary of Perm. (See Figure 6 for the $n=3$ case.)*

Proof. The vertices of the zonotope Z are labeled by proper 2-partitions $\{I_-, I_+\}$ of \hat{n} . They are in one-to-one correspondence with the facets of Perm. It is enough to show

that each vertex sits in the relative interior of the corresponding facet of Perm. A vertex $v_{I_-, I_+} = [x_0, \dots, x_n]$ has homogeneous coordinates

$$(6) \quad x_i = \begin{cases} \pi, & i \in I_+ \\ 0, & i \in I_- \end{cases}$$

Then we see that v_{I_-, I_+} satisfies all inequalities (4), of which exactly one is an equality and the others are strict. \square

2.5. The coamoeba and its skeleton. The image $\mathcal{C} := \mu_2(P) \subset \mathbb{T}^n$ is called the **coamoeba** of P . First, some selected history of the subject: Mikhalkin [Mi04] used Viro's patchworking [Vi83] to construct (torus) fibrations of hypersurfaces via projection to the spine of the amoeba with coamoeba fibers (see also [Vi11], [NS13] and [KZ18]). The intention to have fibers equi-dimensional with full understanding of their geometry is one of the motivations for the present article (see Proposition 5). The first account of the skeleton of the coamoeba as the permutahedron to our knowledge is Futaki-Ueda [FU14]. On the symplectic side Sheridan [Sh11] first made use of the zonotope, the complement of the coamoeba, by viewing its boundary as an immersed Lagrangian sphere in the pair-of-pants. More recently, Nadler-Gammage [GN20] were able to view the skeleton of the coamoeba as a Lagrangian. A different Lagrangian skeleton had previously been given by [RSTZ, Zh18].

When restricted to P_0 , the corresponding part $\mathcal{C}_0 \subset \mathcal{C}$ of the coamoeba is again the hypersimplex $\Delta(2) \subset \Delta_0$, since the only restrictions on the exterior angles α_i in a polygon are $\sum_i \alpha_i = 2\pi$ and $\alpha_i \leq \pi$. In particular, the vertices of \mathcal{C} are labeled by *unordered* 2-partitions $\sigma = \langle I_-, I_+ \rangle$.

We will identify the torus \mathbb{T}^n with $(\mathbb{R}^{n+1}/\mathbb{R})/2\pi\Lambda^*$ where Λ^* is the coweight lattice from the previous section. Let Σ be the image of the *boundary* of Perm in \mathbb{T}^n . Of the $(n+1)!$ vertices of Perm only $n!$ are distinct in \mathbb{T}^n . They correspond to total *cyclic* orderings $\sigma = \langle i_0, \dots, i_n \rangle$. The pairs of opposite facets of Perm are identified, thus giving $2^n - 1$ facets of Σ labeled by (unordered) 2-partitions $\sigma = \langle I_-, I_+ \rangle$. Each contains the corresponding vertex of \mathcal{C} as its barycenter.

More generally, the faces Σ_σ of Σ are labeled by the cyclically ordered partitions $\sigma = \langle I_1, \dots, I_k \rangle$. Thus the face lattice of Σ is dual to the (truncated) lattice of the subdivision $\{\mathbb{T}_\sigma^n : |\sigma| \geq 2\}$ of \mathbb{T}^n . We call the intersection point $\Sigma_\sigma \cap \mathbb{T}_\sigma^n$ the **barycenter** of the face Σ_σ (Σ_σ and \mathbb{T}_σ^n are of complimentary dimensions). We let

$$\gamma_s := \sum_{j=1}^{s-1} |I_j| + \frac{1}{2}|I_s|, \quad s = 1, \dots, k.$$

Then in the homogeneous coordinates θ_i the barycenter of Σ_σ is

$$(7) \quad \frac{2\pi}{n+1} [\underbrace{\gamma_1, \dots, \gamma_1}_{I_1}, \underbrace{\gamma_2, \dots, \gamma_2}_{I_2}, \dots, \underbrace{\gamma_k, \dots, \gamma_k}_{I_k}].$$

(see the interpretation in terms of the distinguished polygons \mathcal{D}_σ below). The vertices ρ_σ^\vee of Σ , cf. (5), are their own barycenters for total orderings $\bar{\sigma}$.

Proposition 4. *The coamoeba \mathcal{C} deformation retracts to its skeleton Σ .*

Proof. This follows from the fact that the interior of the zonotope Z is the complement of the coamoeba and Z sits inside Perm by Proposition 3. \square

For a more profound understanding of Σ it is useful to write down the precise inequalities that cut out the faces of Σ . We start with facets. The hyperplane equality (4) for a facet Σ_{I_-, I_+} reads

$$(8) \quad \frac{(\theta_{i_r} + \cdots + \theta_{i_n})}{s} - \frac{(\theta_{i_0} + \cdots + \theta_{i_{r-1}})}{r} = \pi.$$

We can interpret this as follows. Given a subset $I \subset \bar{n}$, let

$$\theta_I := \frac{1}{|I|} \sum_{i \in I} \theta_i$$

be the **average argument** in I . Then (8) says that the average arguments θ_{I_-} and θ_{I_+} differ by π . The inequalities that cut Σ_{I_-, I_+} are the following. For any subset $I'_- \subseteq I_-$ the average argument $\theta_{I'_-}$ differs from θ_{I_-} by no more than $\frac{\pi}{n+1}(|I_-| - |I'_-|)$, and same for I_+ .

Now we describe the defining conditions for Σ_σ for an arbitrary partition $\sigma = \langle I_1, \dots, I_k \rangle$. Combining the $2^{k-1} - 1$ equations (8) associated to all possible 2-partition coarsenings of σ we arrive at the following set of linear equations:

$$(9) \quad \theta_{I_{s+1}} - \theta_{I_s} = \frac{\pi}{n+1}(|I_s| + |I_{s+1}|), \text{ for all } s = 1, \dots, k.$$

To visualize this condition geometrically it is convenient to introduce a distinguished k -gon \mathcal{D}_σ . Mark $n+1$ equally spaced points on a circle and place let \mathcal{D}_σ be the polygon whose set of vertices is the subset of points that separate the parts in the partition $\sigma = \langle I_1, \dots, I_k \rangle$. Then the equations (9) say that for a point in Σ_σ the average arguments θ_{I_s} are equal to the arguments of the corresponding sides of \mathcal{D}_σ .

The inequalities that bound the face Σ_σ are similar to those for a facet: for any subset $I'_s \subseteq I_s$ the average argument in I'_s differs from θ_{I_s} by no more than $\frac{\pi}{n+1}(|I_s| - |I'_s|)$. The vertices of Σ , which correspond to full partitions $\sigma = \langle i_0, \dots, i_n \rangle$, have arguments of the regular $(n+1)$ -gon.

Remark. There is a striking similarity between the amoeba and the coamoeba worlds. Indeed, when restricted to the simplex Δ_0 the corresponding part $\mathcal{C}_0 \subset \Delta_0$ of the coamoeba looks exactly like the amoeba $\mathcal{A} \subset \Delta$, both are identified with the hypersimplex $\Delta(2)$. But here is a bit of warning. The corresponding part of the skeleton Σ_0 is not the same as the tropical skeleton S . The latter is truly symmetric with respect to all permutations of \hat{n} . On the other hand, Σ_0 retains only the dihedral symmetry of the $(n+1)$ -gon. What we called the barycenters (7) of the faces $\Sigma_\sigma, \sigma \preceq \sigma_0$, are not generally the true barycenters

of the corresponding simplicial faces of Δ_0 . Since $S_3 \cong D_6$ we don't see this distinction in the $n = 2$ case.

3. THE OBER-TROPICAL PAIR OF PANTS AND THE ISOTOPY

3.1. The ober-tropical pair-of-pants and its stratification. Recall that the faces S_{IJ} of S are labeled by pairs $I \subseteq J \subseteq \hat{n}$ and the faces Σ_σ of Σ are labeled by cyclic partitions $\sigma = \langle I_1, \dots, I_k \rangle$ of \hat{n} . Now we define a new object, the **ober-tropical pair-of-pants** \mathcal{P} , as a subcomplex of $S \times \Sigma$:

$$\mathcal{P} := \bigcup_{\sigma, I, J} S_{IJ} \times \Sigma_\sigma,$$

where the union is over all triples $(\sigma, I \subseteq J)$ such that σ divides I . For the $n = 2$ case the ober-tropical pair-of-pants are shown on the right in Fig. 1.

Similar to the cell structure $\{P_{\sigma, J}\}$ of P the stratification $\{\Delta_J \times \mathbb{T}_\sigma^n\}$ of $\Delta \times \mathbb{T}^n$ induces a stratification $\{\mathcal{P}_{\sigma, J}\}$ of \mathcal{P} . As before we will drop the subscript J if $J = \hat{n}$ and denote by \mathcal{P}_0 the stratum corresponding to $\sigma_0 = \{0, 1, \dots, n\}$. Again, since $\{\mathcal{P}_{\sigma, J}\}$ does not touch the vertices of Δ_σ (see (1)) we will view each stratum $\mathcal{P}_{\sigma, J}$ as sitting inside the product of two simplices $\Delta_J \times \Delta_\sigma$. The polyhedral faces of $\mathcal{P}_{\sigma, J}$ are labeled by the pairs $(\tau \preceq \sigma', I \subseteq J')$ such that $\sigma' \preceq \sigma, J' \subseteq J$ and τ divides I . In particular, $\mathcal{P}_{\sigma, J}$ is a subcomplex of $\text{dsd } \Delta_J \times \text{dsd } \Delta_\sigma$.

In the $n = 2$ case we can visualize $\mathcal{P}_0 \subset \mathcal{P} \subset \Delta \times \Delta_0$ as a hexagon in Fig. 7. The entire \mathcal{P}

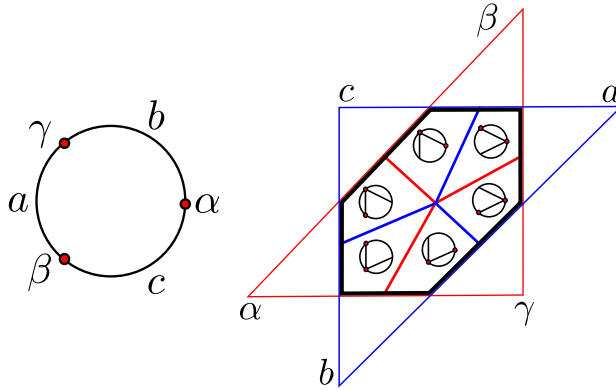


FIGURE 7. The $n = 2$ case: realization of \mathcal{P}_0 as a hexagon made up of 6 squares.

is made up by gluing two of such hexagons along their three (red) sides, as is the classical complex pair-of-pants.

The ober-tropical pair-of-pants \mathcal{P} projects to both skeleta $\mu_1 : \mathcal{P} \rightarrow S$ and $\mu_2 : \mathcal{P} \rightarrow \Sigma$. We would like to describe the generic fibers of both maps. Given a maximal face S_{ij} of S let T_{ij} be the $(n - 1)$ -torus in \mathbb{T}^n defined by $\theta_i = \theta_j$. On the other side, for a maximal face Σ_σ of Σ (that is $\sigma = \langle I_-, I_+ \rangle$ is a 2-partition), let \mathcal{R}_σ be the union of (the closures of) all facets S_{ij} with $i \in I_-, j \in I_+$.

Proposition 5. *The two projections of \mathcal{P} to S and to Σ have $(n - 1)$ -dimensional fibers. The fiber $\mu_1^{-1}(y)$ over a generic point $y \in S_{ij}$ is homotopic to the torus T_{ij} . The fiber $\mu_2^{-1}(s)$ over a generic point $s \in \Sigma_\sigma$ is \mathcal{R}_σ which is an $(n - 1)$ -ball.*

Proof. Since $\dim S_{IJ} = |J \setminus I|$ and $\dim \Sigma_\sigma = n + 1 - |\sigma|$, one easily concludes that the dimension of the fibers in both projections is $n - 1$.

The fiber over a point $s \in \Sigma_\sigma$ is \mathcal{R}_σ by definition. Viro’s patchworking [Vi83] identifies \mathcal{R}_σ with to the closure of the real component of P defined by the choice of coordinate signs according to $\sigma = \langle I_-, I_+ \rangle$. In fact, one can explicitly see that \mathcal{R}_σ is isomorphic to $\text{dsd}(\Delta_- \times \Delta_+)$ as a polyhedral complex.

For $\mu_1^{-1}(y)$ we need to combine the pieces of $\mu_1^{-1}(y)$ from different \mathbb{T}_σ^n ’s. But each $\mu_1^{-1}(y) \cap \mathbb{T}_\sigma^n$ is again, similar to the Viro’s patchworking, is isotopic to the subspace in the simplex Δ_σ defined by $\theta_i = \theta_j$. Combined together they form the torus T_{ij} . \square

Remark. The fibers over generic points in Σ being balls allows one to view \mathcal{P} as the total space of the “cotangent bundle” $T^*\Sigma$ (a symplectic geometer’s dream). Of course, some fibers are singular. For instance, the fiber over any vertex of Σ is the entire S . Still all fibers are contractible which shows that \mathcal{P} contracts to Σ . This is as good as it gets if one wants to follow the philosophy that a symplectic manifold is the “cotangent bundle” over its Lagrangian skeleton.

We will show that \mathcal{P} is, in fact, a topological manifold and the stratification $\{\mathcal{P}_{\sigma,J}\}$ gives it a regular CW-structure. Then, since the two isomorphic regular CW-complexes are homeomorphic, the two versions of pairs-of-pants, complex and ober-tropical, are homeomorphic. The (much stronger) relative version of this homeomorphism is the main result of our paper.

Theorem 6. *The two spaces P and \mathcal{P} are (ambient) isotopic in $\Delta \times \mathbb{T}^n$. An isotopy can be chosen such that it respects the stratification $\{\Delta_J \times \mathbb{T}_\sigma^n\}$.*

The key ingredient for the proof of Theorem 6 is a compatible collection of homeomorphisms between the cell pairs $(\Delta_J \times \Delta_\sigma, P_{\sigma,J})$ and $(\Delta_J \times \Delta_\sigma, \mathcal{P}_{\sigma,J})$. Since any stratum is a face of a maximal stratum, which are all identical, we can restrict to the case $\mathcal{P}_0 \subset \Delta \times \Delta_0$. Using the graphical code, we can identify any subpartition $\sigma \preceq \sigma_0$ with a subset V of marked vertices of the $(n + 1)$ -gon and think of faces Δ_J of Δ as subsets J of marked edges (see Fig. 4). Now the faces of \mathcal{P}_0 are labeled by two pairs $(I \subseteq J, V \subseteq W)$, where I and V are interlacing.

3.2. Unknotted ball pairs. Here we collect some basic results from PL topology which we will need to prove the isotopy. We will be concerned with ball pairs of codimension 2. A ball pair (B^q, B^{q-2}) is **proper** if $\partial B^{q-2} = B^{q-2} \cap \partial B^q$. The **standard ball pair** $B^{q,q-2}$ is the pair of cubes $([-1, 1]^q, \{0, 0\} \times [-1, 1]^{q-2})$. Its boundary is the **standard sphere pair** $S^{q-1,q-3}$. We say that a ball or a sphere pair is **unknotted** if it is homeomorphic to the appropriate standard pair.

Proposition 7. *In the PL category*

- (1) (Levine [Le65] for $q \geq 6$, a surgery argument for $q = 5$ [Ro70], cf. [RS72, Theorem 7.6], and Papakiriakopoulos [Pa57] for $q = 3$.) *A locally flat sphere pair (S^q, S^{q-2}) is unknotted if and only if $S^q \setminus S^{q-2}$ has the homotopy type of a circle.*
- (2) *A proper ball pair (B^q, B^{q-2}) which is a face in an unknotted sphere pair $(\partial B^q, \partial B^{q-2})$ is unknotted and $B^q \setminus B^{q-2}$ has the homotopy type of a circle.*
- (3) (Obvious). *A ball pair (B^{q+1}, B^{q-1}) which is a cone over an unknotted sphere pair (S^q, S^{q-2}) is unknotted.*
- (4) (See, e.g. [RS72, Proposition 4.4]). *A homeomorphism between the boundaries of unknotted balls extends to their interior. Moreover one can choose the extension to agree with any given extension on the subball.*

The first statement is true in TOP for $q \geq 4$, see Freedman [FQ90, Chapter 11] but we could not find a reference for the analog of the second statement in TOP. So to stay on the safe side we will provide a proof for our (B^4, B^2) case “by hand” (see Proposition 11) and remain in the PL category. Similarly, we could not use (1) and (3) for the ober-tropical (B^5, B^3) case and therefore, since an induction argument is involved, neither in any higher dimension. We could run the argument in TOP, but again we decided to do the (B^5, B^3) case by hand (see Lemma 13) and stay in PL. Also we could not find an analogous statement to (1) for the ball pair (which should be true) which might have allowed simpler arguments for some of the statements below.

3.3. Homeomorphism of ball pairs and the proof of Theorem 6. The main building block for the proof of Theorem 6 is a homeomorphism of the pairs $(\Delta_J \times \Delta_\sigma, P_{\sigma,J})$ and $(\Delta_J \times \Delta_\sigma, \mathcal{P}_{\sigma,J})$.

Lemma 8. *Both $(\Delta_J \times \Delta_\sigma, P_{\sigma,J})$ and $(\Delta_J \times \Delta_\sigma, \mathcal{P}_{\sigma,J})$ are proper ball pairs.*

Proof. For the complex pair-of-pants the result was proved in [KZ18, Prop. 5]. In the ober-tropical case we can identify the polyhedral complex $\mathcal{P}_{\sigma,J}$ with the dualizing subdivision of $C_{\sigma,J}^\vee$, the dual polytope of the cyclic polytope, see remark after Proposition 1. \square

Lemma 9. *Both complements $\Delta_J \times \Delta_\sigma \setminus P_{\sigma,J}$ and $\Delta_J \times \Delta_\sigma \setminus \mathcal{P}_{\sigma,J}$ are homotopic to a circle.*

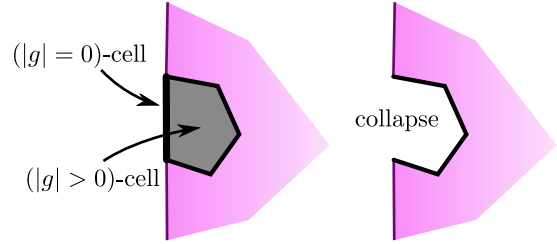
Proof. Let $L_{\sigma,J}$ be the subcomplex of $\Delta_J \times \Delta_\sigma$ consisting of pairs (σ', J') such that σ' does not divide J' . That is $L_{\sigma,J}$ consists of *non-interlacing* pairs (I, V) , where $I \subseteq J$ and V is a subset of the vertices that separate the parts in σ . We claim that both complements in the assertion deformation retract to $|L_{\sigma,J}|$, which then collapses to a circle.

Step 1: $\Delta_J \times \Delta_\sigma \setminus \mathcal{P}_{\sigma,J}$ retracts to $|L_{\sigma,J}|$. Recall that $\mathcal{P}_{\sigma,J}$ is a subcomplex of $\text{dsd } \Delta_J \times \text{dsd } \Delta_\sigma$ which consists of all pairs $(\tau \preceq \sigma', I \subseteq J')$ such that $\sigma' \preceq \sigma$, $J' \subseteq J$ and τ divides I . Its star $\text{Star}(\mathcal{P}_{\sigma,J})$ consists of all pairs $(\tau \preceq \sigma', I \subseteq J')$ such that σ' divides J' . So the complement of $\text{Star}(\mathcal{P}_{\sigma,J})$ in $\Delta_J \times \Delta_\sigma$, which is a deformation retract of $\Delta_J \times \Delta_\sigma \setminus \mathcal{P}_{\sigma,J}$, is the dsd refinement of $L_{\sigma,J}$.

Step 2: $\Delta_J \times \Delta_\sigma \setminus P_{\sigma,J}$ retracts to $|L_{\sigma,J}|$. One may view the complement of the $(n-1)$ -dimensional pair-of-pants in $(\mathbb{C}^*)^n$ as the n -dimensional pair-of-pants. In a similar vein

we represent the complement $N_{\sigma,J}$ of a regular neighborhood of $P_{\sigma,J}$ in $\Delta_J \times \Delta_\sigma$ as the union of k cells $P_{\bar{\sigma},\hat{J}}$, where $\bar{\sigma}$ is a decyclization of $\sigma = \langle I_1, \dots, I_k \rangle$, that is a choice of I_1 , and $\hat{J} = J \cup \{g\}$ contains one additional **ghost** element g . Geometrically, the ghost is $g = -z_0 - \dots - z_n$ and its phase “breaks” the necklace of the I_s . We permit the case $|g| = 0$ but still require g to have a phase in order to represent points in $N_{\sigma,J}$. The full face lattice of the regular CW-complex $N_{\sigma,J}$ is given by $(\hat{\sigma}', J') \preceq (\langle g, \bar{\sigma} \rangle, \hat{J})$ for which $\hat{\sigma}'$ divides J' . Here, $\langle g, \bar{\sigma} \rangle$ refers to the cyclic partition obtained from the decyclization $\bar{\sigma}$ by inserting $\{g\}$ as a new part at the point where σ was broken and then viewing it as a cyclic partition. The case $|g| > 0$ is equivalent to $g \in J'$.

The elements in the face lattice of $N_{\sigma,J}$ decompose into three groups: a) those with $g \notin J'$; b) those with $g \in J'$ and $\hat{\sigma}'$ divides $J' \setminus \{g\}$; c) those with $g \in J'$ and $\hat{\sigma}'$ does not divide $J' \setminus \{g\}$. From an element in b) we may remove g from J' to have an element in a) and this yields a bijection of the sets a) and b). Furthermore the cell with g removed is a facet of the original one and lies in the boundary of $N_{\sigma,J}$. This fact may be used to collapse the cells in a) and b) altogether (inductively starting with the largest-dimensional ones), so that $N_{\sigma,J}$ collapses to its subcomplex consisting of the cells in c), see Figure 8.



In the subcomplex of the cells in c), we combine together all those cells $(\hat{\sigma}', J')$ into a single cell (σ', J') that have the property that removing g from $\hat{\sigma}'$ yields σ' . (The counterclockwise order on the ghost position provides a shelling.) Note that the resulting CW complex is isomorphic to $L_{\sigma,J}$.

FIGURE 8. Collapsing two cells that form a pair under the bijection of a) and b).

Step 3: $|L_{\sigma,J}|$ has the homotopy type of a circle. We first collapse $L_{\sigma,J}$ to a (generally) 2-dimensional subcomplex, the **belt**, which then collapses to a circle (see Fig. 9).

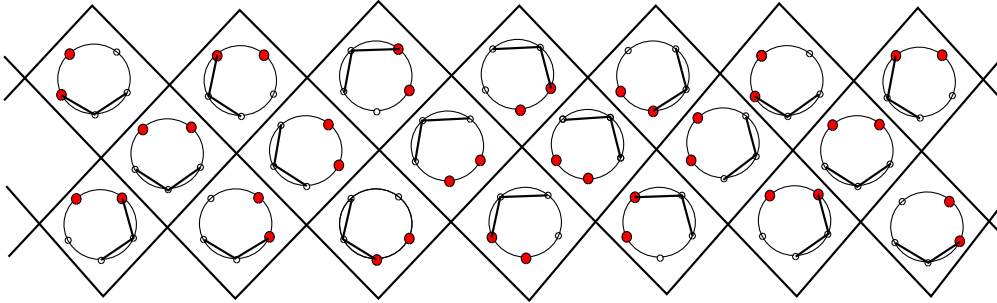


FIGURE 9. The result of collapsing $L_{\sigma,J}$ to its belt for $n + 1 = 5$.

Given a non-interlacing configuration (I, V) we define four integers, the **distances** between I and V , as follows. In the counterclockwise order let v_f be the first vertex in the string of vertices V and v_l be the last vertex. Similar let e_f, e_l be the first and the last

edges in the string of edges. We let k_e be the number of edges in J and k_v be the number of vertices in V between v_l and e_f . Similarly, let m_e, m_v be the numbers of edges in J and vertices in V between e_l and v_f . Note that (I, V) is a face of (I', V') only if their sets (v_f, v_l, e_f, e_l) are the same, or $k'_e \geq k_e, k'_v \geq k_v, m'_e \geq m_e, m'_v \geq m_v$ with at least one inequality strict.

We collapse the intervals $I_{(v_f, v_l, e_f, e_l)}$ of the configurations with fixed sets (v_f, v_l, e_f, e_l) starting from those with $(k_e, k_v, m_e, m_v) = (0, 0, 0, 0)$ and increasing the distances. That is, we collapse $I_{(v_f, v_l, e_f, e_l)}$ after all intervals $I_{(v'_f, v'_l, e'_f, e'_l)}$ with $k'_e \geq k_e, k'_v \geq k_v, m'_e \geq m_e, m'_v \geq m_v$ with at least one inequality strict had been collapsed. Any such interval is either Boolean (then it collapses), or consist of a single element (then it stays). Note that the elements in $I_{(v_f, v_l, e_f, e_l)}$ are faces of its own elements or faces of elements with lower distances (which we collapsed already by induction).

Thus we end up with the subcomplex, which we call the **belt** of $L_{\sigma, J}$, of non-interlacing pairs (I, V) such that I has one or two consecutive elements in J , and V consists of a single vertex or two vertices bounding a part in σ . The belt is a 2-dimensional complex whose 2-faces are squares (see Fig. 9) labeled by consecutive non-interlacing pairs $(v_f$ next to $v_l)$ and $(e_f$ next to $e_l)$, unless $|J| = 2$ or σ consists of just two parts, in which case, either $v_f = v_l$ or $e_f = e_l$, and it is already a circle. The belt has two coordinate directions: in one direction the configuration of edges does not change, in the other direction the vertices are fixed.

Finally we collapse the belt to a circle. It's not as pretty as before since we will have to make a choice between k 's and m 's. We choose k 's and collapse the belt to an 1-dimensional subcomplex $S^1_{\sigma, J}$ (it will be the upper boundary in Fig. 9). The vertices of $S^1_{\sigma, J}$ are pairs (v, e) which are distance $(k_e, k_v) \leq (1, 1)$ apart. The edges of $S^1_{\sigma, J}$ are (V, e) and (v, E) where V is a consecutive pair of vertices and E is a consecutive pair of edges with $(k_e, k_v) = (0, 0)$. So that $|S^1_{\sigma, J}| = S^1$. We collapse the squares one by one starting with $(m_e, m_v) = (0, 0)$ and increasing the distances (m_e, m_v) as we did before. \square

Corollary 10. *The complements of the sphere pairs $\partial(\Delta_J \times \Delta_\sigma) \setminus \partial P_{\sigma, J}$ and $\partial(\Delta_J \times \Delta_\sigma) \setminus \partial \mathcal{P}_{\sigma, J}$ have the homotopy type of a circle.*

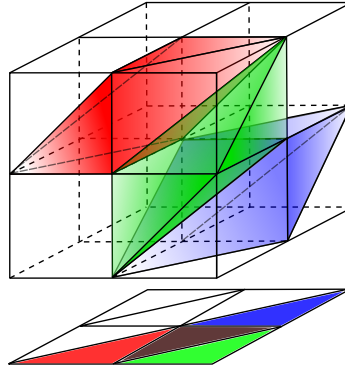
Proof. The complex $L_{\sigma, J}$ which eventually retracts to the circle sits in the boundary of the ball $\Delta_J \times \Delta_\sigma$ in both cases. \square

Proposition 11. *Let $\dim(\Delta_J \times \Delta_\sigma) = 4$. The ball pair $(\Delta_J \times \Delta_\sigma, P_{\sigma, J})$ is unknotted.*

Proof. In the case $\Delta_J^3 \times \Delta_\sigma^1$ there are 4 elements in J and σ is a 2-partition. The 2-ball $P_{\sigma, J}$ is the product $v \times R_\sigma$ where v is the center of the interval Δ_σ^1 and R_σ is the real component of the 2-dimensional pair-of pants, where the elements in J carry plus or minus signs according to which of the two parts of σ they belong. It is easy to trace the image of R_σ in Δ_σ^3 as a 2-disc separating the vertices according to σ . The case $\Delta_J^1 \times \Delta_\sigma^3$ is similar. If σ and J are both of size 3 and *not* maximally interlacing then the ball $P_{\sigma, J}$ in $\Delta_J^2 \times \Delta_\sigma^2$ is the product of two intervals each connecting midpoints of a pair of edges in its own triangle.

The only nontrivial case is the classical one-(complex)-dimensional pair-of-pants: the hexagon P_0 in the product of the 2 triangles $\Delta_0^2 \times \Delta^2$. Similar to the proof of the complement being homotopic to S^1 in Lemma 9, we base our argument on viewing the complement of the 1-dimensional pair-of-pants in $(\mathbb{C}^*)^2$ as the 2-dimensional pair-of-pants. More precisely we represent the complement N_0 of a regular neighborhood of P_0 in $\Delta^2 \times \Delta_0^2$ as the union of three cells $P_{\hat{g}}$, where the position of the ghost g between the cyclically ordered $\{0, 1, 2\}$ is recorded, i.e. $\hat{g} \in \{\{g, 0, 1, 2\}, \{0, g, 1, 2\}, \{0, 1, g, 2\}\}$, see also Figure 10. (As a reminder for clarity: recall that there is a second hexagon which arises from the other cyclic ordering $\{0, 2, 1\}$ and which also sits inside three 4-balls giving the total of six strata as discussed in the $n = 3$ case of Figure 3.)

FIGURE 10. Thinking of $\Delta^2 \times \Delta_0^2$ as the union of three 4-dimensional cells $P_{\hat{g}}$ which project to these octahedra in the argument factor of $(\mathbb{C}^*)^3$.



The boundary of the regular neighborhood of P_0 decomposes naturally as $SP_0 \cup ((\partial P_0) \times B^2)$ where SP_0 is a trivial circle bundle over P_0 and B^2 is a disc. To show that the proper ball pair $P_0 \subset \Delta_0^2 \times \Delta^2$ is unknotted, it suffices to show that there exists a homeomorphism $N_0 \xrightarrow{\sim} SP_0 \times [0, 1]$ where we like to require the homeomorphism to restrict to the identity on $SP_0 \times \{0\}$ in the sense that we have SP_0 naturally be part of the boundary of N_0 .

We define $W_{\hat{g}} := SP_0 \cap P_{\hat{g}}$ and will show $W_{\hat{g}}$ is a three-ball for each \hat{g} . Since N_0 is glued from the three 4-balls $P_{\hat{g}}$, in order to find the required homeomorphism $N_0 \xrightarrow{\sim} SP_0 \times [0, 1]$ we may instead show for each \hat{g} that $P_{\hat{g}}$ is homeomorphic to $W_{\hat{g}} \times [0, 1]$ in such a way that their gluing respects the product decomposition. We will call $W_{\hat{g}}$ a **wedge**. The boundary of each wedge decomposes into two squares and one hexagon and the squares are where a wedge meets the other wedges, that is, the wedges have identical shape and glue as shown in Figure 11.

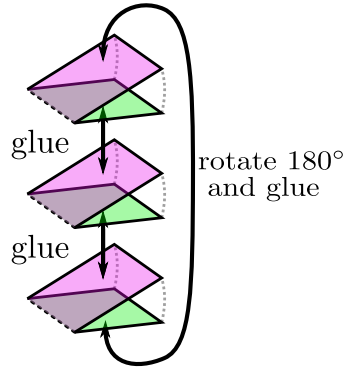


FIGURE 11. The three $W_{\hat{g}}$ and how they glue to give SP_0 .

We now construct the desired homeomorphism $P_{\hat{g}} \xrightarrow{\sim} W_{\hat{g}} \times [0, 1]$. We start off by analyzing the structure of the polytopes $P_{\hat{g}}$. Recall that the faces of $P_{\hat{g}}$ are indexed by graphical code,

that is by interlacing subsets of the circle with four distinct points on it and the arcs between the points labeled according to \hat{g} in clockwise order. In particular, there are 8 facets in each $P_{\hat{g}}$, given by unmarking either a vertex or an arc while everything else is marked. Each $P_{\hat{g}}$ has a special facet given by unmarking the ghost and this facet is $W_{\hat{g}}$ because unmarking the ghost means setting $g = 0$, i.e. $z_0 + z_1 + z_2 = 0$ however the phase of g is still recorded having the effect of $W_{\hat{g}}$ being inside SP_0 rather than P_0 itself. We pictorially explain in Figure 12 that the intersection of two $P_{\hat{g}}$ is a facet of each. Indeed, note that when a vertex

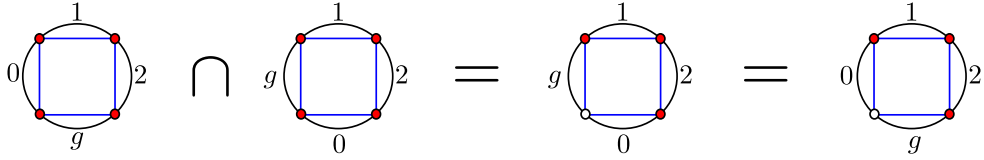


FIGURE 12. Computing $P_{\{g,0,1,2\}} \cap P_{\{0,g,1,2\}}$ in graphical code.

is unmarked, the adjacent labels don't have a preferred order since they lie in the same I_j . In summary, each $P_{\hat{g}}$ has three types of facets: 1) $W_{\hat{g}}$, 2) two facets that connect it with the two other $P_{\hat{g}}$ and 3) five further facets characterized by that the ghost and each of its adjacent vertices are marked. Nonetheless, all eight facets of each $P_{\hat{g}}$ are isomorphic and look like the polytope in the center of Figure 13.

An important fact is that all three $W_{\hat{g}}$ meet in a disjoint union of three edges. We call them **special edges** and their graphical code is given on the right in Figure 13 (and the edges are bold). The figure shows $W_{\{g,0,1,2\}}$ in the center and explains on the right how $W_{\{g,0,1,2\}}$ gets identified with the wedge that we introduced before, i.e. with a 3-ball whose boundary decomposes in two squares and one hexagon. The original hexagonal face on top of $W_{\{g,0,1,2\}}$ becomes a square so that the special edges it contains lie opposite to one another - similarly for the bottom face. The remaining part of the boundary becomes a hexagon in the process. Convincing ourselves that the illustration on the left of Figure 13 accurately depicts how $W_{\{g,0,1,2\}}$, $W_{\{g,0,1,2\}}$ and $W_{\{g,0,1,2\}}$ glue together, we have thus verified the structure of SP_0 as glued by wedges claimed in Figure 11.

In the following, we will use the terminology of “square” (respectively “hexagon”, etc.) either to refer to actual squares (or hexagons, etc.) or to polyhedral complexes that glue to 2-cells whose boundary decomposes into 4 (or 6) intervals. For instance, the hexagonal top face in the middle of Figure 13 is a square in the sense that its homeomorphic image in the wedge is a square. Similarly, the complement of the two actually hexagonal faces of the polytope in the middle is a “hexagon” in the sense that its homeomorphic image in the wedge is a hexagon.

To finish the proof, we are going to exhibit for each $P_{\hat{g}}$ a second copy $W'_{\hat{g}}$ of a wedge in its boundary disjoint from $W_{\hat{g}}$. We will show that each $P_{\hat{g}}$ is PL homeomorphic to $W_{\hat{g}} \times [0, 1]$ where $W_{\hat{g}} \times \{0\}$ is the original $W_{\hat{g}}$ and $W_{\hat{g}} \times \{1\}$ is the extra copy; furthermore the gluing of the $P_{\hat{g}}$ will respect the product structure.

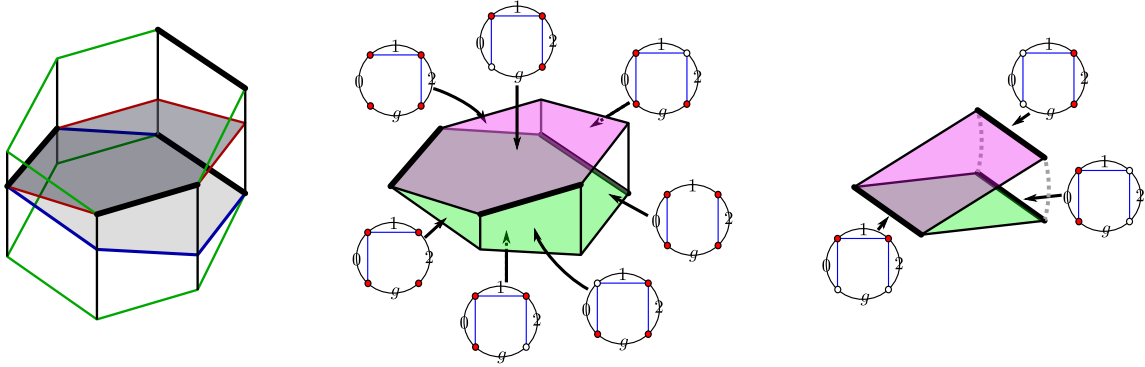


FIGURE 13. The middle shows $W_{\{g,0,1,2\}}$ with each facet labeled by its graphical code and special edges marked bold. The right shows the homeomorphic version of it as a wedge with the special edges labeled by their graphical code. The left shows $W_{\{0,g,1,2\}}$ (top), $W_{\{g,0,1,2\}}$ (middle) and $W_{\{0,1,g,2\}}$ (bottom) and the top and bottom face of the resulting hexagonal prism shall be identified by translation to give SP_0 , cf. Figure 11.

We first observe that the “opposite end” of N_0 , complementary to SP_0 , is a Moebius strip. To be precise, the union of faces of all $P_{\hat{g}}$ that do not meet any $W_{\hat{g}}$ forms the following strip where the left and right non-bold boundary edges get identified according to the endpoint labels.

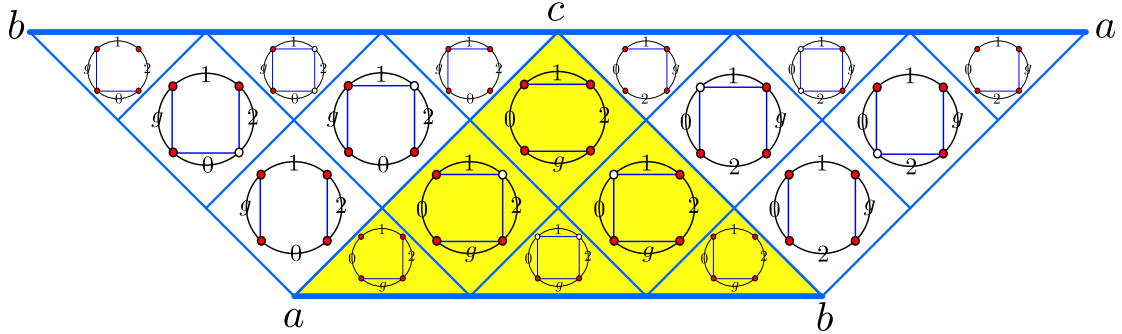


FIGURE 14. The Moebius strip of cells in N_0 that are disjoint from SP_0 .

The strip decomposes into three triangles, each of which lies in one $P_{\hat{g}}$. The center triangle in the figure (yellow) is contained in $P_{\{g,0,1,2\}}$, the left one in $P_{\{0,g,1,2\}}$ and the right one in $P_{\{0,1,g,2\}}$. Focusing on a single $P_{\hat{g}}$ now, we next need to understand better its facets that meet the corresponding triangle of the strip. Recall that the facets fall into three groups. The group characterized by having the ghost and its adjacent vertices marked consists of five facets. To understand how these glue together, consider the left of Figure 15 that shows these facets partially glued to a hexagonal tower. An additional gluing has to be carried out which affects the back side of the tower, a square shown in the middle of Figure 15. The square decomposes into two triangles along the (bold) diagonal.

The dashed triangle gets glued to the solid triangle resulting in a (blue) triangle which is precisely the triangle that is part of the Moebius strip. The result of the gluing is shown on the right in Figure 15, let's call it the **blob**.

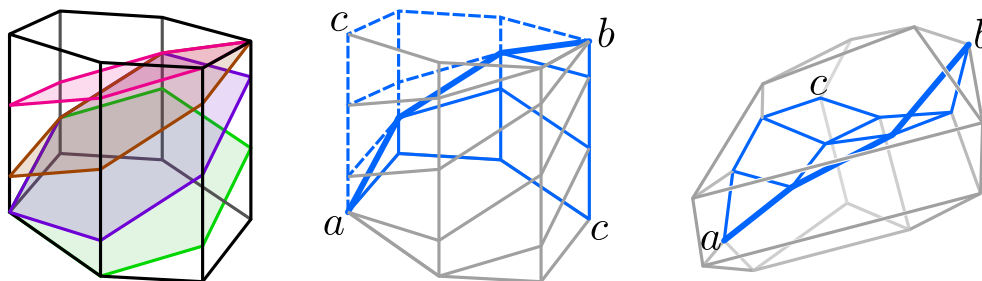


FIGURE 15. The five facets of $P_{\{g,0,1,2\}}$ that each meet the (blue) triangular part of the Moebius strip in a union of 2-cells. The situation looks similar for the other $P_{\hat{g}}$ after changing the labels a, b, c appropriately.

We next place a wedge around the triangle inside the blob. Figure 16 depicts how this is going to work. The two squares of the wedge are the intersection of the wedge with the boundary of the blob and depicted on the left. The hexagonal face of the wedge is not shown to not overburden the illustration. It *wraps around* the blue triangle, so that the resulting wedge - let us call it $W'_{\hat{g}}$ - contains the blue triangle in the way depicted in the middle of Figure 16.

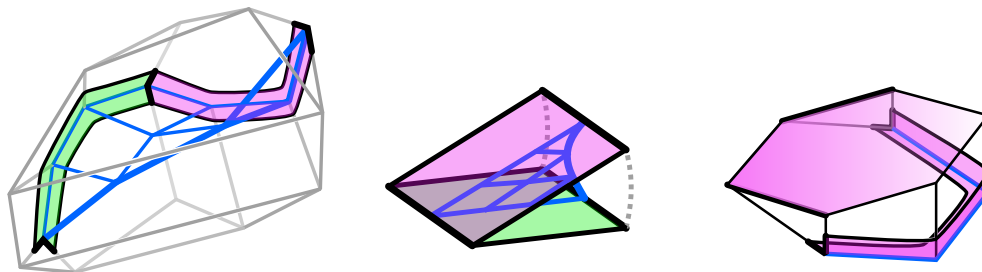


FIGURE 16. The wedge $W'_{\hat{g}}$ in the blob, containing the blue triangle (left and middle). The right shows one of three 3-cells that are the intersection of two $P_{\hat{g}}$'s.

Most importantly, we can decompose the blob into the wedge $W'_{\hat{g}}$ and $H \times [0, 1]$ where H is the hexagonal face of $W'_{\hat{g}}$ (the one that is not depicted). The next important observation is that the union of those faces of the blob (right of Figure 15) which do *not* meet the blue triangle is precisely the complement of the two hexagonal facets in the boundary of $W_{\hat{g}}$. In other words, the union of the blob and $W_{\hat{g}}$ (with their natural gluing) is a copy of two wedges ($W_{\hat{g}}$ and $W'_{\hat{g}}$) glued along $H \times [0, 1]$ so that $W_{\hat{g}}$ meets $H \times [0, 1]$ in $H \times \{0\}$ and $W'_{\hat{g}}$ meets $H \times [0, 1]$ in $H \times \{1\}$. Next recall the facets of $P_{\hat{g}}$ that are also contained in

the neighboring 4-cells. We depict one of these on the right of Figure 16 with the purpose of illustrating how it contains two (pink) squares: one that it has in common with $W_{\hat{g}}$ (in hexagonal form) and the other being the matching square of $W'_{\hat{g}}$. We observe that we may view the facet as $S \times [0, 1]$ where $S \times \{0\}$ is the pink (hexagonal) square of $W_{\hat{g}}$ and $S \times \{1\}$ is the pink square of $W'_{\hat{g}}$.

Note that we have just given a PL homeomorphism of the boundary of $P_{\hat{g}}$ and the boundary of $W_{\hat{g}} \times [0, 1]$. Any such homeomorphism can be extended to the interiors (e.g. by taking stars), so we have found a homeomorphism $P_{\hat{g}} \xrightarrow{\sim} W_{\hat{g}} \times [0, 1]$ for each \hat{g} . By construction, these homeomorphisms are compatible with gluing the three $P_{\hat{g}}$ so that we have constructed the desired PL homeomorphism $N_0 \xrightarrow{\sim} SP_0 \times [0, 1]$. \square

Proposition 12. *Let $\dim(\Delta_J \times \Delta_\sigma) \neq 4$. The ball pair $(\Delta_J \times \Delta_\sigma, P_{\sigma,J})$ is unknotted.*

Proof. First we check that the pair $(\Delta_J \times \Delta_\sigma, P_{\sigma,J})$ is locally flat. Consider the map

$$\phi : \Delta_J \times \Delta_\sigma \rightarrow \mathbb{C}, \quad (z_0, \dots, z_n) \mapsto z_0 + \dots + z_n.$$

By an argument similar to the proof of [KZ18, Proposition 5] one concludes that for small $|t| \leq \epsilon$ the fiber $\phi^{-1}(t)$ is a closed ball. In particular, $\phi^{-1}(0) = P_{\sigma,J}$ and the map ϕ exhibits the product structure in a small neighborhood of $P_{\sigma,J} \subseteq \Delta_J \times \Delta_\sigma$.

As a consequence we conclude that the sphere pair $(\partial(\Delta_J \times \Delta_\sigma), \partial P_{\sigma,J})$ is locally flat. Then by combining Corollary 10 and part (1) of Proposition 7 we conclude that the sphere pair $(\partial(\Delta_J \times \Delta_\sigma), \partial P_{\sigma,J})$ is unknotted except in dimension (S^4, S^2) .

Finally we can view $(\Delta_J \times \Delta_\sigma, P_{\sigma,J})$ as a facet of a one-dimension higher polytope (just add a *ghost* element to \hat{n}) and run the above argument for this one-higher dimensional case. Now the result follows from part (2) of Proposition 7. \square

Remark. Unfortunately the map $\phi : \Delta_J \times \Delta_\sigma \rightarrow \mathbb{C}$ above does not behave well at the boundary of its image. Namely the fibers $\phi^{-1}(t)$ for $|t| = 1$ are generally lower dimensional and not balls. For example in the (B^4, B^2) -case (cf. Proposition 11) the preimage of the entire circle $|t| = 1$ is the Moebius band. Otherwise that would give a quick and easy proof of the unknotness.

No inductive argument is needed here, contrary to the ober-tropical case below. Combining the two Propositions 11 and 12 we get the unknotness for all pairs $(\Delta_J \times \Delta_\sigma, P_{\sigma,J})$.

Lemma 13. *Let $\dim(\Delta_J \times \Delta_\sigma) \leq 5$. The ball pair $(\Delta_J \times \Delta_\sigma, P_{\sigma,J})$ is unknotted.*

Proof. For $\dim(\Delta_J \times \Delta_\sigma) \leq 3$ the statement is trivial. For $\dim(\Delta_J \times \Delta_\sigma) = 4$ the 2-ball is the cone over the circle in S^3 which is unknotted since its complement is homotopic to S^1 by Corollary 10. For $\dim(\Delta_J \times \Delta_\sigma) = 5$ the cases $\Delta_J^4 \times \Delta_\sigma^1$ and $\Delta_J^1 \times \Delta_\sigma^4$ are easily reduced to just one factor as in the beginning of the proof of Proposition 11. Similar reduction happens for not maximally interlacing $\Delta_J^3 \times \Delta_\sigma^2$ and $\Delta_J^2 \times \Delta_\sigma^3$. Thus the only non-trivial case to consider is $\Delta_J^3 \times \Delta_\sigma^2$ where J and σ are maximally interlacing. The other case $\Delta_J^2 \times \Delta_\sigma^3$ is similar.

Let σ be a 3-partition $\langle I_1, I_2, I_3 \rangle$ and let $J = \{0, 1, 2, 3\}$ split its elements, say, as $0, 1 \in I_1$, $2 \in I_2$, $3 \in I_3$. We list the maximal faces of $\mathcal{P}_{\sigma, J}$ (we will omit the J part from the subscript of the faces S_{IJ} and denote the 3 coarsenings of σ as $a = \langle I_1 \cup I_2, I_3 \rangle$, $b = \langle I_1, I_2 \cup I_3 \rangle$, $c = \langle I_3 \cup I_1, I_2 \rangle$):

$$\begin{aligned} S_{23} \times \Sigma_a, S_{03} \times \Sigma_a, S_{13} \times \Sigma_a, \\ S_{03} \times \Sigma_b, S_{13} \times \Sigma_b, S_{02} \times \Sigma_b, S_{12} \times \Sigma_b, \\ S_{02} \times \Sigma_c, S_{12} \times \Sigma_c, S_{32} \times \Sigma_c. \end{aligned}$$

Notice that the face S_{01} is not present and one can combine the faces S_{0x} and S_{1x} into a

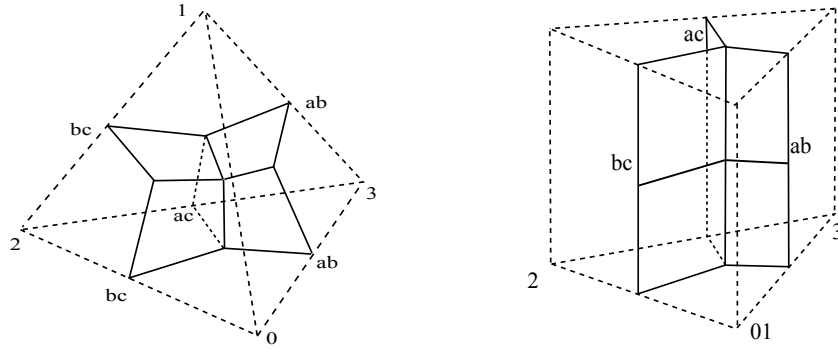


FIGURE 17. The S -part of the complex $\mathcal{P}_{\sigma, J}$ with Σ_{xy} -fibers labeled.

single cell. Now it is easy to see that the entire complex $\mathcal{P}_{\sigma, J}$ is a subdivision of the (properly subdivided at the boundary) complex $\mathcal{P}_{\sigma, \bar{J}} \times [0, 1]$ (see Figure 17), where in \bar{J} we treat 0 and 1 as a single element. Moreover this PL homeomorphism extends to the ambient balls, that is, the pair $(\Delta_J \times \Delta_\sigma, \mathcal{P}_{\sigma, J})$ is homeomorphic to the pair $(\Delta_{\bar{J}} \times \Delta_\sigma, \mathcal{P}_{\sigma, \bar{J}}) \times [0, 1]$. \square

Proposition 14. *The ball pair $(\Delta_J \times \Delta_\sigma, \mathcal{P}_{\sigma, J})$ is unknotted.*

Proof. We will do the induction on dimension of the strata $\Delta_J \times \Delta_\sigma$. For $\dim(\Delta_J \times \Delta_\sigma) \leq 5$ we have Lemma 13. In general, $(\Delta_J \times \Delta_\sigma, \mathcal{P}_{\sigma, J})$ is a cone pair over its boundary. So that its unknotness (and hence the local flatness) follows from unknotness of the boundary pair $(\partial(\Delta_J \times \Delta_\sigma), \partial\mathcal{P}_{\sigma, J})$ by applying part (3) of Proposition 7. To show that the boundary pair $(\partial(\Delta_J \times \Delta_\sigma), \partial\mathcal{P}_{\sigma, J})$ is unknotted we apply part (1) of Proposition 7. The complement is homotopic to the circle by Corollary 10, the local flatness within the relative interiors of the strata of $\Delta_J \times \Delta_\sigma$ is by induction.

The only thing which remains to show is that $\mathcal{P}_{\sigma, J}$ is locally flat at a stratum $\Delta_{J'} \times \Delta_{\sigma'} \subseteq \Delta_J \times \Delta_\sigma$. Note that each face S_{IJ} of S at the stratum $\Delta_{J'}$, $I \subseteq J' \subseteq J$, is locally the product $(S_{IJ} \cap \Delta_{J'}) \times \text{Cone}_{JJ'}$, where $\text{Cone}_{JJ'}$ is the relative cone of Δ_J at its face $\Delta_{J'} \subseteq \Delta_J$. Similarly, any face of Σ_σ is locally a product $(\Sigma_\sigma \cap \Delta_{\sigma'}) \times \text{Cone}_{\sigma\sigma'}$. Thus the entire pair $(\Delta_J \times \Delta_\sigma, \mathcal{P}_{\sigma, J})$ at $\Delta_{J'} \times \Delta_{\sigma'}$ is locally the product of the pair $(\Delta_{J'} \times \Delta_{\sigma'}, \mathcal{P}_{\sigma', J'})$ with the cone $\text{Cone}_{JJ'} \times \text{Cone}_{\sigma\sigma'}$ and the local flatness follows by induction from a lower dimension. \square

Proof of Theorem 6. Propositions 12 and 14 provide homeomorphisms of ball pairs $(\Delta_J \times \Delta_\sigma, P_{\sigma,J})$ and $(\Delta_J \times \Delta_\sigma, \mathcal{P}_{\sigma,J})$ which respect the stratifications. By the Alexander trick, the homeomorphisms are homotopic to the identity on all cells. An inductive application of Proposition 7 part (4) on strata gives an isotopy which respects the stratification. \square

REFERENCES

- [Ca17] R. Caputo. *The isotopy problem for the phase tropical line*. Beitr Algebra Geom (2019), doi:10.1007/s13366-019-00456-9
- [CBM09] R. Castaño Bernard, D. Matessi. *Lagrangian 3-torus fibrations*. J. Differential Geom. **81** (2009), 483–573.
- [Er94] R. M. Erdahl. *Zonotopes, Dicings, and Voronoi’s Conjecture on Parallelehedra*. European Journal of Combinatorics, Volume 20, Issue 6 (1999), 527–549.
- [EM19] J.D. Evans, M. Mauri. *Constructing local models for Lagrangian torus fibrations*. arXiv:math/1905.09229.
- [FQ90] M. Freedman and F. Quinn. *Topology of 4-manifolds*. Princeton Mathematical Series. 39. Princeton, NJ, 1990.
- [FU14] M. Futaki, K. Ueda. *Tropical coamoeba and torus-equivariant homological mirror symmetry for the projective space*. Comm. Math. Phys. **332**(1) (2014), 53–87.
- [GKZ94] I. Gelfand, M. Kapranov, and A. Zelevinsky. *Discriminants, resultants, and multidimensional determinants*. Birkhäuser Boston, Inc., Boston, MA, 1994.
- [GN20] B. Gammage, D. Nadler. *Mirror symmetry for honeycombs*. Trans. Amer. Math. Soc. 373(1) (2020), 71–107.
- [G01] M. Gross. *Topological mirror symmetry*. Inv. Math., volume 144 (2001), 75–137.
- [GS06] M. Gross, B. Siebert. *Mirror symmetry via logarithmic degeneration data I*. J. Differential Geom. **72** (2006), 169–338.
- [KZ18] G. Kerr and I. Zharkov. *Phase tropical hypersurfaces*. Geometry & Topology 22 (2018), 3287–3320.
- [Le65] J. Levine. *Unknotting spheres in codimension 2*. Topology, 4 (1965), 9–16.
- [Mi04] G. Mikhalkin. *Decomposition into pairs-of-pants for complex algebraic hypersurfaces*. Topology Vol. 43 (2004), Issue 5, 1035–1065.
- [NS13] M. Nisse and F. Sottile. *Non-Archimedean coamoebae*, in *Tropical and non-Archimedean geometry*. 73-91, Contemp. Math. 605, Amer. Math. Soc. 2013.
- [Pa57] C. D. Papakiriakopoulos. *Dehn’s lemma and the asphericity of knots*. Ann. Math. 66 (1957), 1–26.
- [RSTZ] H. Ruddat, N. Sibilla, D. Treumann, E. Zaslow. *Skeleta of affine hypersurfaces* Geom. Topol. 18(3), (2014), 1343–1395.
- [RZ20] H. Ruddat and I. Zharkov. *Topological SYZ fibrations*. In preparation.
- [Ro70] C. P. Rourke. *Embedded handle theory, concordance and isotopy*. Topology of manifolds, Ed. by Cantrell and Edwards, 431–438. Chicago: Markham, 1970.
- [RS72] C. P. Rourke and B. J. Sanderson. *Introduction to Piecewise-Linear Topology*. Springer-Verlag, 1972.
- [Sh11] N. Sheridan. *On the homological mirror symmetry conjecture for pairs of pants* J. Diff. Geom. 89(2), 271–367.
- [St19] R. Stanley. *Private communications*.
- [SYZ96] A. Strominger, S.T. Yau, E. Zaslow: *Mirror symmetry is T-duality*, Nuclear Physics B **479** (1996), 243–259.

- [Vi83] O. Viro. *Gluing algebraic hypersurfaces and constructions of curves*. Tezisy Leningradskoj Mezh-dunarodnoj Topologicheskoy Konferencii 1982, Nauka (1983), 149-197 (Russian). English trans-lation of the main chapter in *Patchworking Real Algebraic Varieties*, arXiv:math/0611382.
- [Vi11] O. Viro. *On basic concepts of tropical geometry*. Trudy Mat. Inst. Steklova, vol. 273, (2011), No. 1, 271-303.
- [Zi95] G. Ziegler. *Lectures on Polytopes*. Springer-Verlag, New York 1995.
- [Zh18] P. Zhou. *Lagrangian skeleta of hypersurfaces in $(\mathbb{C}^*)^n$* . arXiv:math.SG/1803.00320

JOHANNES GUTENBERG-UNIVERSITÄT MAINZ & UNIVERSITÄT HAMBURG
E-mail address: `ruddat@uni-mainz.de`, `helge.ruddat@uni-hamburg.de`

KANSAS STATE UNIVERSITY, 138 CARDWELL HALL, MANHATTAN, KS 66506
E-mail address: `zharkov@ksu.edu`